Composites with Micro- and Nano-Structure

Computational Methods in Applied Sciences

Volume 9

Series Editor

E. Oñate
International Center for Numerical Methods in Engineering (CIMNE)
Technical University of Catalunya (UPC)
Edificio C-1, Campus Norte UPC
Gran Capitán, s/n
08034 Barcelona, Spain
onate@cimne.upc.edu
www.cimne.com

Vladimir Kompiš

Composites with Micro- and Nano-Structures

Computational Modeling and Experiments

Springer

Vladimir Kompiš

Academy of the Armed Forces
Liptovský Mikuláš
Slovakia

ISBN 978-1-4020-6974-1 e-ISBN 978-1-4020-6975-8

Library of Congress Control Number: 2008928508

Printed on acid-free paper

9 8 7 6 5 4 3 2 1

springer.com

Contents

Introduction

This book contains selected, extended papers presented (with three exceptions) in the thematic ECCOMAS conference on **Composites with Micro- and Nano-Structure (CMNS) – Computational Modelling and Experiments** held in Liptovský Mikuláš, Slovakia, in May 28–31, 2007 and sponsored by the Slovak Ministry of Education.

Composite materials play important role in all mechanical, civil as well as in electrical engineering structures especially in the last two decades in connection with the nano-materials and nano-technologies. Of course the chemical engineering is a connecting element for all these applications.

Computational methods and experiments are a basis for the Simulation-Based Engineering Science (SBES). SBES can play a remarkable role in promoting the developments vital to health, security and technological competitiveness of nations.

Recent experimental and computational results demonstrate that materials reinforced with stiff particles and fibres can obtain substantial improvements in stiffness, thermal conductivity and electro-magnetic properties. Materials reinforced with fibres can have very different properties in different directions. The material can have very good conductivity in one direction and can be isolator in other directions. Most important reinforcing materials discovered less than 20 years ago, which are in the centre of interest in many universities and research institutions are the carbon nano-tubes.

With these new materials also importance of computational simulations and experimental verifications increases.

The book contains 16 papers:

The first paper, by Leung et al., employs an atomic-scale finite element method to study torsion buckling of single-walled carbon nano-tubes (SWNTs). The dependence of critical torsion angle on the length is discussed and compared with conventional shell theory. Strain energy and morphologies of the SWNT are discussed.

In the second paper, the authors study the structure and mechanical strength properties of Cu nano particulate aggregates. The inter-particle interaction models have

been considered to account the long-range forces: electrostatic, van der Waals and coupled Johnson, Kendall and Roberts (JKR) and Brownian force models. The assemblies considered have poly-size distribution of particles.

In the third paper the interaction of matrix with fibres and fibre with other fibres in the fibre-reinforced composites (FRC) is numerically simulated using 1D continuous source functions along the fibre axis and 2D source functions inside the ends of fibres. Numerical examples show that the interaction of the end parts of fibres is crucial for evaluation of the mutual interaction of fibres in the composite. Correct simulation of all parts is important for evaluation of stiffness and strength of the FRC.

In the fourth paper the effective dynamic material properties for materials with microstructure are assumed. Micro-scale inertia are taken into account and numerical homogenization is performed. The frequency dependent macroscopic material parameters are found for frequency range from 0 up to 1 MHz.

The fifth paper describes modelling of diffusive and massive phase transformation of a multi-component system based on the principle of maximum dissipation rate by Onsager; the finite thickness of the interface between both phases can be respected. The mathematical analysis results in an initial-value problem for a system of partial differential equations of evolution with certain non-local integral term; the unknowns are the mole fractions of particular components.

Paper number six deals with numerical implementation of local integral equation formulation of 2D linear elastic media with continuous variable Young's modulus. Two meshless presentations of the formulation are described and accuracy, convergence and numerical stability are investigated.

The seventh paper presents methods for the modelling of the processes that accompany obtaining and use of powder nano-composites. For this purpose, a number of physical-mathematical models, including the models of obtaining of nano-sized powders at "up down" processes, the models of the main steps of powder nano-composites compaction and the models of deformation of powder nano-composites under the ambient action were developed.

The eighth paper presents the basis of the nano-impact test and the idea of prediction of fracture occurrence, especially fatigue behaviour of nano-impacted materials. Finite element (FE) model is applied to identification of the material model of hard nano-coating in the multilayer system. In the second part of the chapter a new approach to analysis of fracture phenomena is introduced as the fatigue criteria, which are used in simulation of nano-impact test. Results of simulations with the fatigue criteria implemented into the FE code for the analysed problem are discussed.

The ninth paper contains a description of a continuum micromechanics model development and experimental validation of strand-based engineering wood products aimed to improve the mechanical properties of wood products. The model allows considering of the relevant (micro-) characteristics of the wood on the mechanical properties of panels.

The tenth paper focuses on experimental investigations and numerical modelling of micromechanical behaviour of cement paste taken as a fundamental representative of building materials with heterogeneous microstructure. The experimental

nano-indention and its implications to evaluation of material properties are focused. Better descriptions of indentation based on analytical visco-elastic solution and finite element model with general visco-elasto-plastic constitutive relation are proposed. These models are used for simulation of indentation and for estimation of material parameters at micrometer scale.

Paper number eleven studies the prediction of the crack growth of the ductile fracture of forgets steel 42CrMo4. Crack extension is simulated in sense of element extinction algorithm based on the damage model Gurson-Tvergard-Needleman and on the cohesive zone model. Determination of micro-mechanical parameters is based on the combination of static tests, microscopic observation and numerical calibration procedures by FEM.

In the twelfth paper a longitudinal polynomial continuous variation of the stiffness properties is considered in the stiffness matrix of the beam element and presented for the analysis of the electric, thermal and structural field. The transversal and longitudinal variation of the material properties is considered.

In the thirteenth paper a novel computational modal and solution procedure are proposed for inhomogeneous materials with the eigenstrain formulation of the boundary integral equations. Each inhomogeneity embedded in the matrix with various shapes and material properties described via the Eshelby tensors can be obtained through either analytical or numerical means. As the unknowns appear only on the boundary of the solution domain, the solution scale of the inhomogeneity problem with the present model is greatly reduced. To enhance further the computational efficiency, the overall elastic properties using the present model with eigenstrain formulation are solved using the newly developed boundary point method for particle reinforced inhomogeneous materials over a representative volume element.

The fourteenth paper deals with reliability of porous ceramics based on experimentation and analysis. Damage prior to rupture and aging because of corrosive activity in porous materials is discussed. Fracturing processes in the material that result to rupture under pore pressure are studied on the micro-scale by the numerical simulation model.

Finally, in the last paper a computational framework for extracting effective diffusivities from micro-tomographic images is presented. Effective diffusivity of a cement paste whose microstructure has been digitized is derived, consistent homogenization and statistical testing and interpretation of results are highlighted.

I would like to thank my colleague Dr. Štiavnický for his help in preparation of the book.

Vlado Kompiš

Chapter 3
Method of Continuous Source Functions for Modelling of Matrix Reinforced by Finite Fibres

Vladimír Kompiš, Mário Štiavnický, Marián Kompiš, Zuzana Murčinková, and Qing-Hua Qin

Abstract Fibres are the most effective reinforcing material. Simulation of the interaction of matrix with fibres and fibre with other fibres is a most important problem for understanding the behaviour of fibre-reinforced composites (FRC). Large gradients in all displacement, stress and strain fields and their correct simulation for near and far field action are essential for effective computational modelling. Because of the large aspect ratios in fibre type reinforcing particles, methods using volume discretization are not efficient. Source functions (forces, dipoles, dislocations) describe correctly both near and far field activities and thus help to simulate all interactions very precisely. The method of continuous source functions allows us to satisfy the continuity of fields between very stiff fibres and much more flexible matrix by 1D continuous functions along the fibre axis and local 2D functions in the end parts of a fibre with only few parameters. Two types of examples with rows of non-overlapping sheets of fibre and with overlapping fibres show that the interaction of the end parts of fibres is crucial for evaluation of the mutual interaction of fibres in the composite. Correct simulation of all parts is important for evaluation of stiffness and strength of the FRC.

Vladimír Kompiš and Mário Štiavnický
Academy of the Armed Forces of General M.R. Štefánik, Liptovský Mikuláš, Department of Mechanical Engineering, Slovak Republic
kompis@aoslm.sk

Marián Kompiš
Siemens Program and System Engineering s.r.o., 01001 Žilina, Slovakia
marian.kompis@siemens.com

Zuzana Murčinková
Department of Technical Devices Design, Faculty of Manufacturing Technologies of Technical University Košice with seat in Prešov, Slovakia
murcinkova@kryha.sk

Qing-Hua Qin
Department of Engineering, Australian National University, Canberra ACT 0200, Australia
qinghua.qin@anu.edu.au

V. Kompiš (ed.), *Composites with Micro- and Nano-Structure – Computational Modeling and Experiments.*

3.1 Introduction

Composites of the future will offer many advances over those in use today. Composite materials reinforced by fibres are important materials possessing excellent mechanical and also thermal and electro-magnetic properties. The outstanding properties of mechanical strength of carbon nano-tubes (CNT) are well known. This allows them to be used as possible reinforcing materials [1]. Reinforcement with nano-tubes facilitates the production of very strong and light materials. These properties of CNTs have attracted the attention of scientists all over the world. Understanding the behaviour of such composite materials is essential for structural design. Computational simulations play an important role in this process [25].

In computational simulations, boundary-type solution methodologies are now well established as alternatives to prevailing domain-type methods such as FEM [3, 33], because of the computational advantages they offer by way of reduction of dimensionality, good accuracy for the whole domain, and simplicity of data preparation for the model. The BEM [2, 5] is the most popular and efficient boundary solution procedure, formulated in terms of boundary integral equations (BIEs). In BEM the integral identities are applied over elements discretizing the boundary of the domain.

However, the use of elements in the BEM, with evaluation of weakly singular, strongly singular, hyper-singular and quasi-singular integrals, is a cumbersome and non-trivial task. The integration of elements containing singularity requires special integration models. If a singularity is close to the element (i.e. the element with quasi-singularity), then the integrals with large gradients in points closest to the singularity must be computed by high order quadratures, or by another special technique in order to obtain good accuracy.

The boundary contour method (BCM) [20, 22] represents an effort to improve efficiency by transferring the surface integrals into line integrals by application of Stokes' theorem for 3D problems.

The boundary node method (BNM) [21, 32] is a combination of the moving least squares (MLS) approximation scheme and the standard BIE method. This method divorces the traditional coupling between spatial discretization (meshing) and interpolation as commonly practised in the FEM or in the BEM. Instead, a "diffuse" approximation, based on MLS approximants, is used to represent the unknown functions and surface cells, with a very flexible structure used for integration. Thus, the BNM belongs with boundary meshless methods.

Using the virtual boundary method and radial basis functions (RBF), the boundary point collocation method has been proposed to construct a boundary meshless formulation [29, 31], in which the boundary conditions and body forces are enforced and coupled with the analogue equation method to construct a boundary-type meshless method for analysing nonlinear problems [30].

Hybrid-Trefftz methods [8, 12, 15, 27] are also boundary-type methods. They use a set of trial functions, singular or non-singular, which *a priori* satisfy the corresponding linear part of the governing differential equation inside the (sub)domain

(the large element). Other independent functions maintain the continuity between the subdomains (in a weak and strong sense).

The method of fundamental solutions (MFS) [9, 14] is a boundary meshless method which does not need any mesh. In linear problems, only nodes (collocation points) on the domain boundaries and a set of source functions (fundamental solutions) in points outside the domain are necessary to satisfy the boundary conditions. MFS has certain advantages over the BEM, as it completely avoids the need for any integral evaluation and it leads to very simple formulations in some problems. However, large numbers of both collocation points and source functions are necessary if the shape of the domain is complex and moreover, the resulting system of equations is bad conditioned in some problems. The source functions serve as the trial functions and must be placed outside the domain. The location of the source functions is vital to both the accuracy and the numerical stability of the solution. The MFS can be also included among Trefftz-type methods.

A novel boundary-type meshless method – the boundary point method (BPM) was developed in [18]. The BPM is based on the direct formulation of conventional and hypersingular BIEs employing favourable features of both the MFS and BEM. It is well known that for the integration of kernel functions over boundary elements, the shorter the distance between the source and field points, the more difficult it is to evaluate them accurately because of the properties of the fundamental solutions. In the formulation, "moving elements" are introduced by organizing relevant adjacent nodes in order to describe the local features of a boundary such as position, curvature and direction, over which the treatment of singularity and integration can be carried out, a benefit not only for the evaluation of integrals in the case of coincidence points, but also for the versatility afforded by using unequally spaced nodes along the boundary.

In special problems like composite materials reinforced with short micro-/nanofibres, all the methods mentioned above require very many elements or boundary points to obtain a sufficiently accurate solution. In such problems the materials of the matrix and fibres have very different electro-magneto-thermo-mechanical properties and very large gradients are present in all fields in matrix and in fibres as well. Domain formulations also require billions of equations after numerical discretization to simulate the decaying effects with increasing distance from the fibre and the gradients along the boundaries. Boundary formulations can simulate the decaying effect well, but they also require a large number of equations to simulate the large gradients on the inter-domain boundaries. Both near and far field effects are important. Near field effects are important for evaluation of the strength of the composite and far fields are important for correct evaluation of the stiffening effect.

The fast multi-pole method (FMM) [11] was developed to increase the efficiency of numerical models. A FMM based on the Taylor expansion of kernel functions (the fast multipole boundary integral equation method (FMBIEM)) [7, 10, 19, 23, 24, 26] was developed to solve the problem of composite materials reinforced by many small particles, considerably accelerating BEM solutions. However, near field integrals still have to be solved by classical BEM and the boundaries are also discretized by elements.

In this paper, a novel method of continuous source functions (MCSF) for the modelling of problems such as composites reinforced with short fibres is presented. The source functions (forces and dipoles [4]) are continuously distributed along the fibre axis (i.e. outside of the domain) and their intensity is modelled by 1D quadratic elements along the axis. Moreover, 2D distribution of the source functions are used to satisfy the continuity in the end part of the fibre. The method can be included among BPMs, as inter-domain continuity is satisfied in the discrete points of the inter-domain boundary in the least squares (LS) sense. The model presents a significant reduction (even by several orders) in the resulting system of equations compared to FEM, BEM, and other known mesh reducing methods. The MCFS requires integration over 1D and 2D elements. Analytic integration using symbolic manipulation is used for evaluation of the quasi-singular integrals occurring in the models, and it is a very efficient tool for the evaluation of such integrals. Numerical integration is used for 2D elements because of complex form of the integrands. Recently a procedure of improved efficiency for such problems was also developed [18]. If the source domain and the field point (e.g. the collocation point) are far from each other, the source values can be replaced by their resulting value and the computation is again considerably reduced. The effect is similar to that used in the FMBIEM but the algebraic manipulation is simpler, based on the principles of mechanics in this case instead of the Taylor expansion used in FMBIEM.

The model is applied to simulation of the interaction of matrix-fibre-fibre for regularly distributed straight fibres in a patch inside the matrix. Two different problems are studied: (1) fibres distributed in rows without overlap of the fibres and (2) with overlap of the fibres.

3.2 Modelling of Composite Material Reinforced with Short Fibers

Let us consider a linear elastic material reinforced by regularly distributed “short” straight fibres. Let the cross sectional dimensions of a fibre be much smaller than its length, the tensional (axial) stiffness of the fibre is much higher than the stiffness of the matrix and ideal cohesion between the matrix and the fibres is assumed in the present model. Then a continuity condition between the matrix and a fibre can be introduced by zero strains (rigid fibre) in the longitudinal direction along the fibre boundary and by zero difference of the displacements in each pair of points on opposite fibre boundaries in the perpendicular direction to the fibre axis.

If the fibres are straight then an alternative continuity condition can be expressed by the difference between displacements of a point on the fibre surface and a point in the middle cross-section along the fibre axis.

All displacement, strain and stress fields are split into a homogeneous part corresponding to constant stress and strain acting in the matrix without the fibres and local fields corresponding to the stiffening effect. For simplicity, isotropic material properties are assumed in this paper.

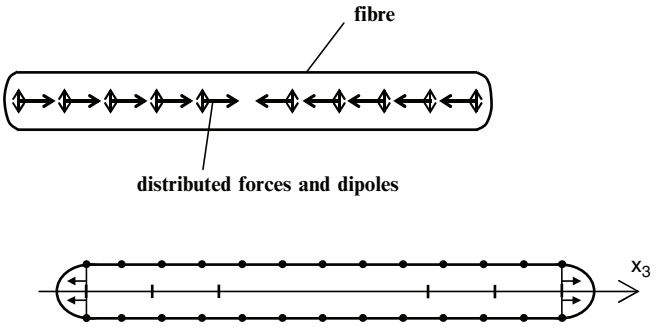

Fig. 3.1 Fibre-matrix interaction simulated by source functions placed inside the fibre (the numbers indicate 1D elements)

The interaction of the matrix and a fibre is simulated by source functions placed inside the fibre along its axis. The source functions are continuous forces and dipoles (Fig. 3.1) acting outside the domain (matrix).

The field of displacements in an elastic continuum caused by a unit force acting in the direction of the axis x_p is given by the Kelvin solution as it is known from BEM [2, 5, 6]

$$U_{pi}^{(F)} = \frac{1}{16\pi G(1-\nu)} \frac{1}{r} \left[(3-4\nu)\, \delta_{ip} + r_{,i} r_{,p} \right] \tag{3.1}$$

where i denotes the x_i coordinate of the displacement, G and ν are shear modulus and Poisson's ratio of the material of the matrix. δ_{ij} is the Kronecker's delta and r is the distance between the source point s, where the force is acting and a field point t, where the displacement is expressed, i.e.

$$r = \sqrt{r_i r_i},\ r_i = x_i(t) - x_i(s) \tag{3.2}$$

with the summation convention over repeated indices and

$$r_{,i} = \partial r / \partial x_i(t) = r_i / r \tag{3.3}$$

is its directional derivative.

The gradients of the displacement fields are the corresponding derivatives of the field (3.1) at the point t

$$U_{pi,j}^{(F)} = -\frac{1}{16\pi G(1-\nu)} \frac{1}{r^2} \left[(3-4\nu)\, \delta_{pi} r_{,j} - \delta_{pj} r_{,i} - \delta_{ij} r_{,p} + 3 r_{,i} r_{,j} r_{,p} \right] \tag{3.4}$$

The second derivative of nth power of the radius vector is defined as

$$\left(r_{,k}^{n} \right)_{,j} = r_{,kj}^{n} = \frac{n}{r} \left(r_{,k}^{n-1} \delta_{jk} - r_{,j} r_{,k}^{n} \right) \tag{3.5}$$

The strains are

$$E_{pij}^{(F)} = \frac{1}{2}\left(U_{pi,j}^{(F)} + U_{pj,i}^{(F)}\right) = -\frac{1}{16\pi G(1-\nu)}\frac{1}{r^2}$$
$$\left[(1-2\nu)\left(\delta_{pi}r_{,j} + \delta_{pj}r_{,i}\right) - \delta_{ij}r_{,p} + 3r_{,i}r_{,j}r_{,p}\right] \tag{3.6}$$

and the stress components ij of this field are

$$S_{pij}^{(F)} = 2GE_{pij}^{(F)} + \frac{2G\nu}{1-2\nu}\delta_{ij}E_{pkk}^{(F)} = \frac{1}{8\pi(1-\nu)}\frac{1}{r^2}$$
$$\left[(1-2\nu)\left(\delta_{ij}r_{,p} - \delta_{jp}r_{,i} - \delta_{ip}r_{,j}\right) - 3r_{,i}r_{,j}r_{,p}\right] \tag{3.7}$$

The displacement field of a dipole can be obtained from the displacement field of a force by differentiating it in the direction of the acting force, i.e.

$$U_{pi}^{(D)} = U_{pi,p}^{(F)} = -\frac{1}{16\pi G(1-\nu)}\frac{1}{r^2}\left[3r_{,i}r_{,p}^2 - r_{,i} + 2(1-\nu)r_{,p}\delta_{ip}\right] \tag{3.8}$$

The summation convention does not apply over the repeated indices p here or in the following relations. Recall that the derivatives in the direction perpendicular (see, Eq. (3.4)) to the force define a force couple [4, 13], which can be also used in some problems. These derivatives have the physical meaning of corresponding couples of forces acting at a point.

The gradients of a dipole displacement field (3.8) are

$$U_{pi,j}^{(D)} = -\frac{1}{16\pi G(1-\nu)}\frac{1}{r^3}\left[-15r_{,i}r_{,j}r_{,p}^2 + 3r_{,i}r_{,j}\right.$$
$$\left. +2(1-2\nu)\,\delta_{ip}\left(\delta_{jp} - 3r_{,j}r_{,p}\right) + 6r_{,i}r_{,p}\delta_{jp} + \delta_{ij}\left(3r_{,p}^2 - 1\right)\right] \tag{3.9}$$

and corresponding strain and stress fields are

$$E_{pij}^{(D)} = \frac{1}{2}\left(U_{pi,j}^{(D)} + U_{pj,i}^{(D)}\right) = -\frac{1}{16\pi G(1-\nu)}\frac{1}{r^3}\left[-15r_{,i}r_{,j}r_{,p} + 3r_{,i}r_{,j}\right.$$
$$+2(1-2\nu)\,\delta_{ip}\delta_{jp} + 6\nu\left(\delta_{ip}r_{,j}r_{,p} + \delta_{jp}r_{,i}r_{,p}\right)$$
$$\left. +\,\delta_{ij}\left(3r_{,p}^2 - 1\right)\right] \tag{3.10}$$

$$S_{pij}^{(D)} = 2GE_{pij}^{(D)} + \frac{2G\nu}{1-2\nu}\delta_{ij}E_{pkk}^{(D)} = -\frac{1}{8\pi(1-\nu)}\frac{1}{r^3}\left[(1-2\nu)\left(2\delta_{ip}\delta_{jp} + 3r_{,p}^2\delta_{ij} - \delta_{ij}\right)\right.$$
$$\left. +6\nu r_{,p}\left(r_{,i}\delta_{jp} + r_{,j}\delta_{ip}\right) + 3\left(1 - 5r_{,p}^2\right)r_{,i}r_{,j}\right] \tag{3.11}$$

If unit forces acting at source points (i.e. the fundamental solution satisfying the homogeneous equilibrium equations in the whole domain with the exception of the source point alone) are located in discrete points outside the solution domain for computational models, and also the collocation points (i.e. the points at which the boundary conditions have to be satisfied) are chosen at some discrete points

of the domain boundary, then the method of solution is known as the method of fundamental solutions (MFS) [9, 14]. This method is very simple. It does not need any elements or any integration and thus is a fully meshless method. These functions are Trefftz functions and they serve as interpolators in the whole domain. Note that any other Trefftz functions can be used for this purpose [15].

On the other hand, dipoles are very effective tools for the modelling of composites reinforced by spherical or ellipsoidal particles [16, 28], and if the density of particles is small a single triple dipole can very effectively simulate a particle. The efficiency of the model is higher than that using the FMBIEM [7, 10, 19, 23, 24, 26] as integration is not necessary. Note that a dipole located inside a particle, i.e. outside of the domain represented by the matrix, gives both zero resulting force and moment along the particle boundary and thus the global equilibrium is not destroyed by local errors, as it can be when using MFS [15]. However, the location of the source points is vital for the best simulation of continuity and equilibrium along interdomain boundaries.

However, if the fibres are thin then satisfaction of continuity of displacements, strains and tractions on the surface between the matrix and fibres and corresponding displacements and strains along the fibre would require a very large number of source points to simulate the interaction. Moreover, in the end parts of a fibre the fields have very large gradients [17], which increases the difficulties with accuracy and numerical stability of the solution.

In our models, continuous distribution of source points is used for simulation of the interaction. This method is here called the method of continuous source functions (MCSF). It is possible to use both distributed forces and distributed dipoles along the fibre axis (1D distribution) and oriented in the axis direction in the model. Their role is mainly to satisfy continuity in the fibre axis direction. Continuity in directions perpendicular to the fibre axis is served mainly by the continuous dipoles along the fibre axis, but directed perpendicularly to the fibre axis. Recall that continuously distributed dipoles are derivatives of continuously distributed forces.

The ends of a fibre can be in the form of half spheres or cylinders. It is important to satisfy the boundary conditions (b. c.) in these parts also. Without taking these b. c. into account, the source functions located along the fibre axis can give incorrect results in evaluation of the stiffening effect. Special b. c. have to be specified for tube-type particles such as carbon nanotubes. Instead of displacements, zero tractions must be prescribed in such cases.

The distribution is approximated by piecewise quadratic functions with C^0 continuity between the elements. The following integrals need to be evaluated

$$\int_a^b \frac{x_s^n \left(x_s - x_f\right)^p}{\left(y^2 + x_s - x_f^2\right)^{\frac{m}{2}+r}} dx_s = f\left(x_f\right) \tag{3.12}$$

where x is the coordinate along the fiber axis, the subscripts s and f denote the source and field point and exponents n, m, p and r are integer numbers. y is the distance of the field point from the axis. The integral (3.12) is transformed for better manipulation to

$$\int_{a+x_f}^{b+x_f} \frac{\left(x+x_f\right)^n x^p}{\left(y^2+x^2\right)^{\frac{m}{2}+r}} dx = f\left(x_f\right) \tag{3.13}$$

The integrands are quasi-singular with very large local gradients and they are evaluated analytically by symbolic manipulation in MATLAB.

Quadratic elements were chosen as the best way of approximation by polynomial functions. It was found that they can better approximate the b. c., as the end parts of fibres transmit the largest forces from the matrix and it was preferable to use large gradients in these parts of fibres when small elements were used for the parts with large gradients than to use larger elements of high order polynomials. Although the integrals give large gradients at the ends of fibres, i.e. if $x_f \to a$, or $x_f \to b$, the C^0 continuity of elements permits a smooth solution to be obtained.

3.3 Numerical Results and Discussion

Two different problems were simulated in order to study the interaction of fibres with matrix and also the interaction of fibres: (1) a patch of non-overlapping rows of fibres as shown in Fig. 3.2, and (2) a patch of overlapping rows of fibres according to the Fig. 3.3. In the examples the modulus of elasticity of the matrix was $E = 1{,}000$ and the Poisson ratio $\nu = 0.3$. The matrix was reinforced by a patch of straight rigid cylindrical fibres. The length of fibres was L = 100 and L = 1,000 and the radius

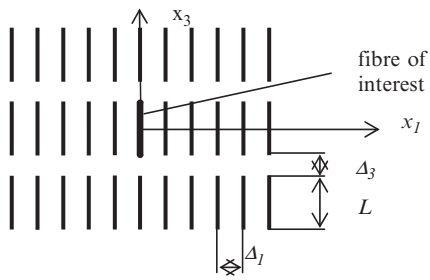

Fig. 3.2 Patch of non-overlapping rows of fibres

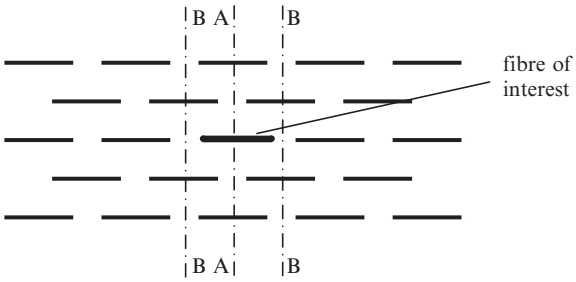

Fig. 3.3 Patch of overlapping rows of fibres

R = 1. The distance between fibres was $\Delta_1 = \Delta_2 = \Delta_3 = 16$ and for longer fibres also $\Delta_3 = 200$ in the fibre direction. The fibres in the patch contained approximately 1% of the volume of the composite material.

The patches of fibres consisted of $5 \times 5 \times 7$ fibres in the presented examples and the "fibre of interest" (FOI) was chosen in the centre to study the interaction of the fibre with matrix and with the other fibres as well. The domain is assumed to be loaded by far field stress $\sigma_{33\infty} = 10$ in the direction (x_3), which is also parallel to fibres' axes. The model of the fibre used in these examples contained fewer than 100 unknown parameters (intensities of the source functions) and about 200 collocation points. The problem is solved by the least squares (LS) method.

In order to reduce the number of unknown parameters it was assumed that the intensities of source functions are identical in all fibres. That is of course not correct, as the fibres at the patch boundaries will transmit larger loads than those in the middle. An iterative procedure can be used to correct the simulation. But for the purpose of quantitative evaluation of the influence of fibre reinforcement the models give sufficient information.

Some results are presented in the next figures. All displacement, strain and stress fields given in the figures are the local components of corresponding fields. Recall that the far fields have to be added in to obtain the total quantities.

Figures 3.4–3.10 show the local fields in the vicinity of the fibre of interest (the coordinates' origin is in the middle of the fibre) for L = 1,000 R with overlay and the distance $\Delta_3 = 200$R. Displacement differences of the points on the fibre boundary were linear along the fibre (Fig. 3.4). As the LS method was used in the procedure, the errors were examined as shown in Figs. 3.4 and 3.5. The circles denote nodal

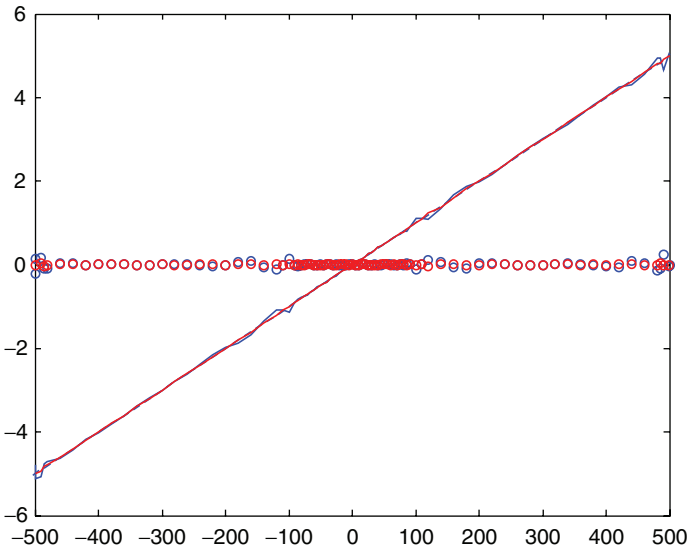

Fig. 3.4 Local displacements along a fibre (L = 1,000R)

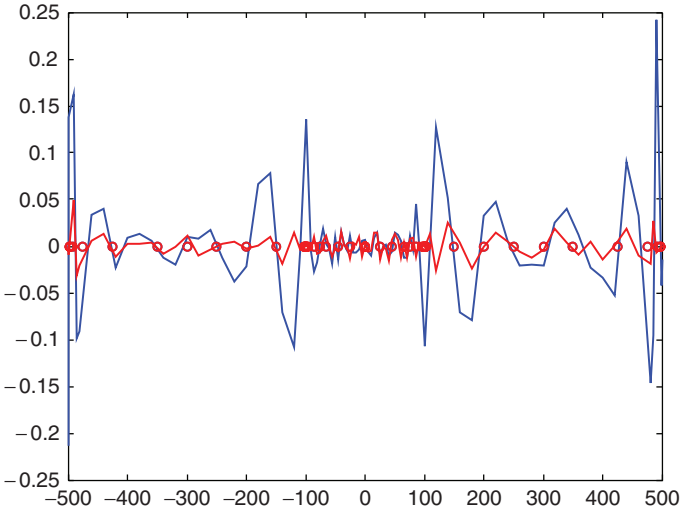

Fig. 3.5 Errors in local displacements along fibre (L = 1,000 R)

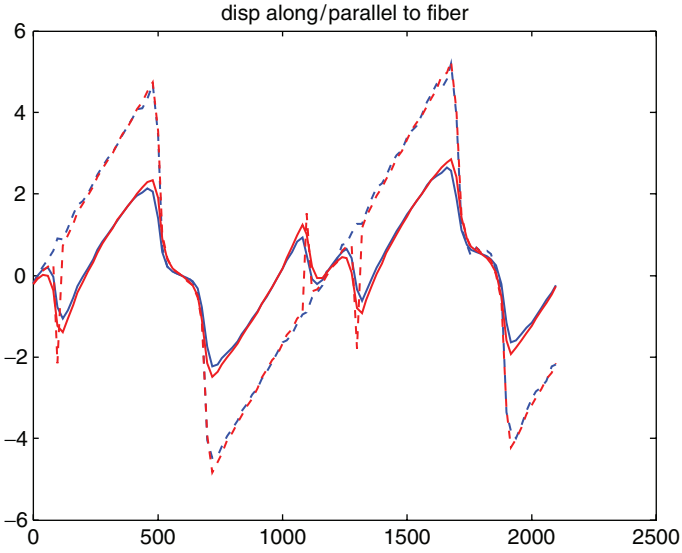

Fig. 3.6 Displacement field parallel to fibre axis (L = 1,000 R)

points in distributed source functions (fictive forces of the Kelvin functions and dipoles) along the fibre axis. Two different models were used: one with discontinuities (A – red) near the ends of neighbouring fibres where the fields have large gradients, and one with continuous distribution of source functions (B – blue) along whole fibre axis.

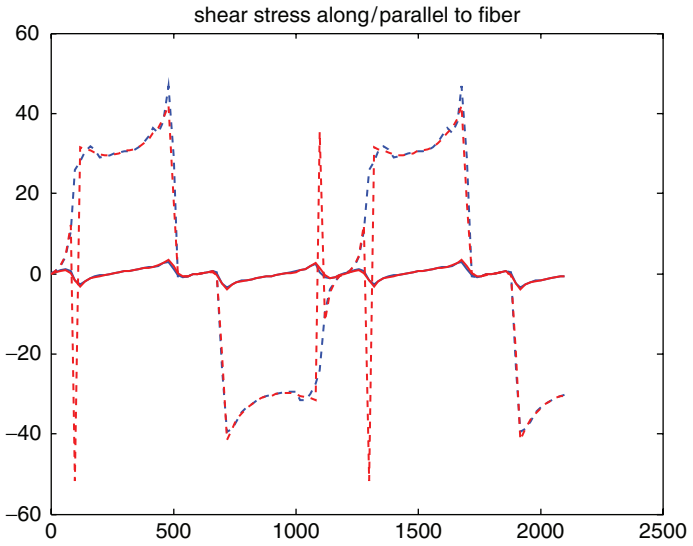

Fig. 3.7 Shear stress parallel to fibre axis (L = 1,000 R)

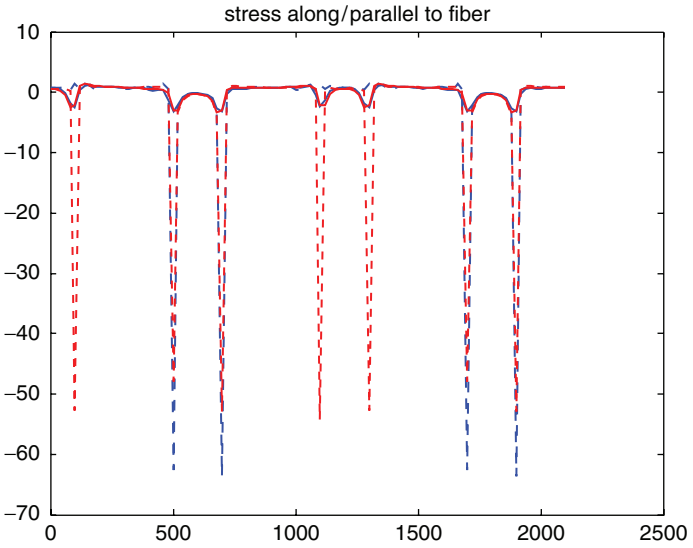

Fig. 3.8 Stress in fibre direction parallel to fibre axis (L = 1,000 R)

Displacements, shear stresses and stresses in the fibre direction along the fibre (dashed line) and in the middle between the fibre of interest and the neighbouring fibre are shown in Figs. 3.6–3.8, respectively. Figures 3.9 and 3.10 contain the distribution of intensities of fictive forces along the fibre and the forces in the fibre cross section given by the integral of forces. The discontinuous model contains large local

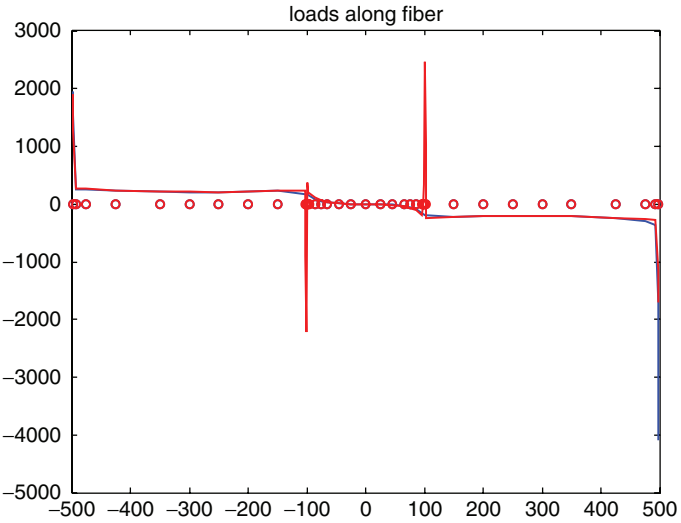

Fig. 3.9 Intensity of fictive forces along fibre (L = 1,000R)

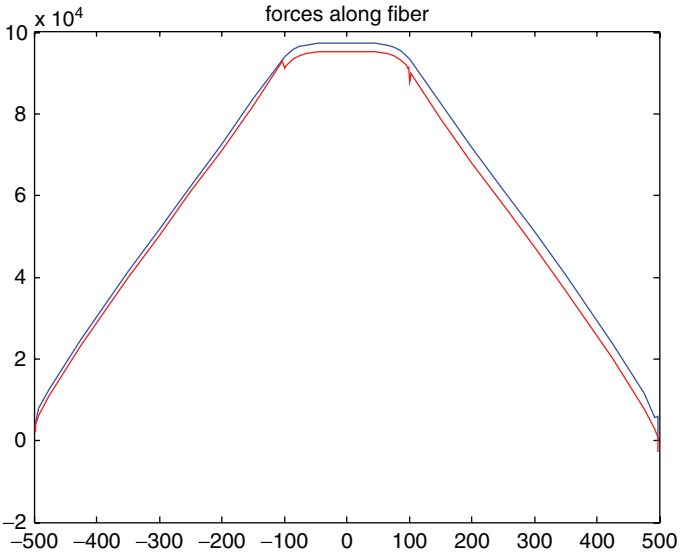

Fig. 3.10 Forces in fibre cross section (L = 1,000R)

forces in the vicinity of the discontinuities. The maximal forces in the middle of the fibre are important for evaluation of the strength of the fibre. Both continuous and discontinuous models give similar results and the difference in maximal values is less than 3%.

Figure 3.11 shows the influence of both the gap between the fibres and the overlap for longer fibres. As could be expected, the configuration with overlap gives a much larger reinforcing effect. The fictive forces are concentrated at the end parts of fibres only in the case without overlap of fibres (Fig. 3.12). A configuration without overlap can occur when long fibres are broken by large forces.

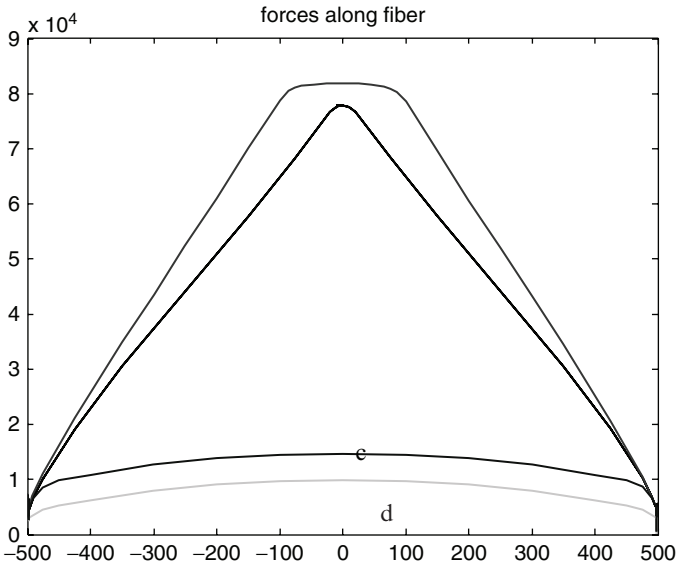

Fig. 3.11 Forces in fibre cross section with overlap $\Delta_3 = 200$ R (red), $\Delta_3 = 16$ R (black); without overlap $\Delta_3 = 200$ R (cyan), $\Delta_3 = 16$ R (blue) by (L = 1,000 R)

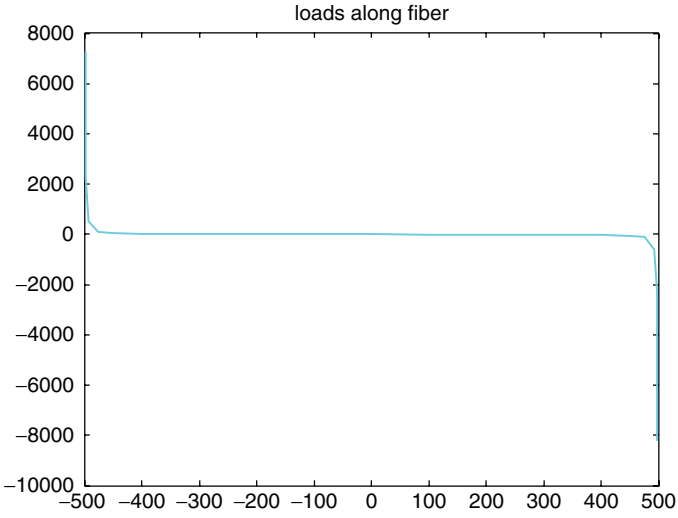

Fig. 3.12 Intensity of fictive forces along fibre in without overlap (L = 1,000 R)

Different transmission of load between matrix and fibres in the cases with and without overlap can be observed in shorter fibres (L = 100R), as can be seen from Figs. 3.12–3.19. The forces in the fibres with overlap are greater than without overlap, but the difference is not as great as occurs with longer fibres.

Two aspects are important for accurate simulation in computational models: (1) how accurately the compatibility conditions in the inter-domain (matrix-fibre)

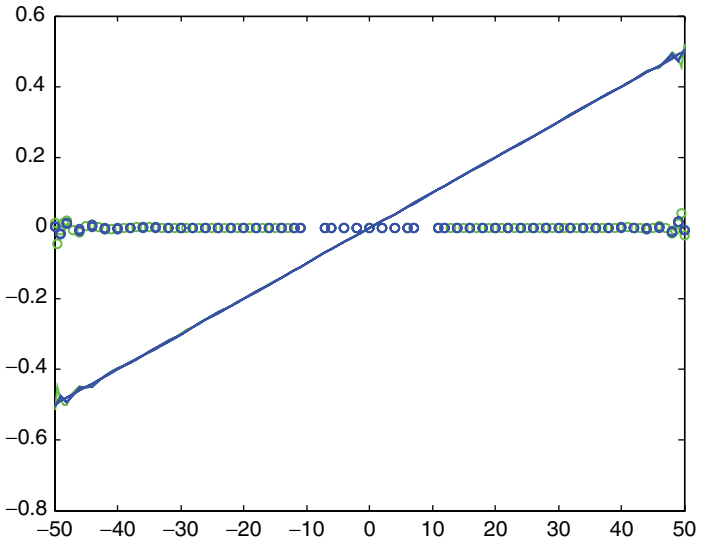

Fig. 3.13 Local displacements along a fibre (L = 100R)

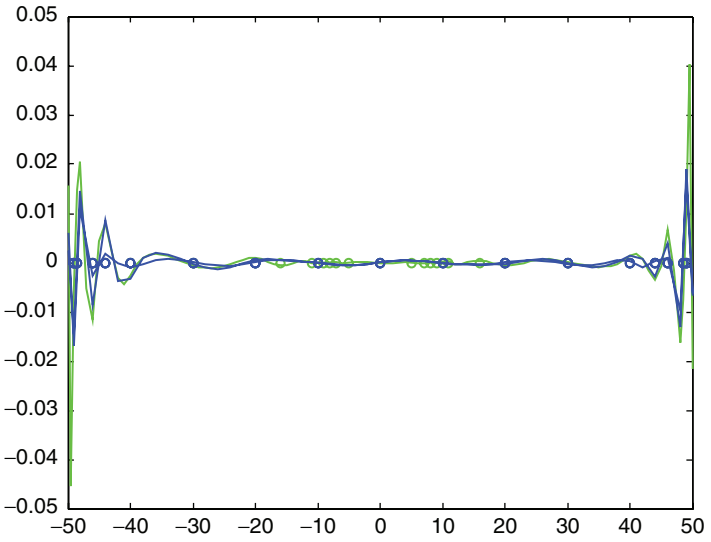

Fig. 3.14 Errors in local displacements along fibre (L = 100R)

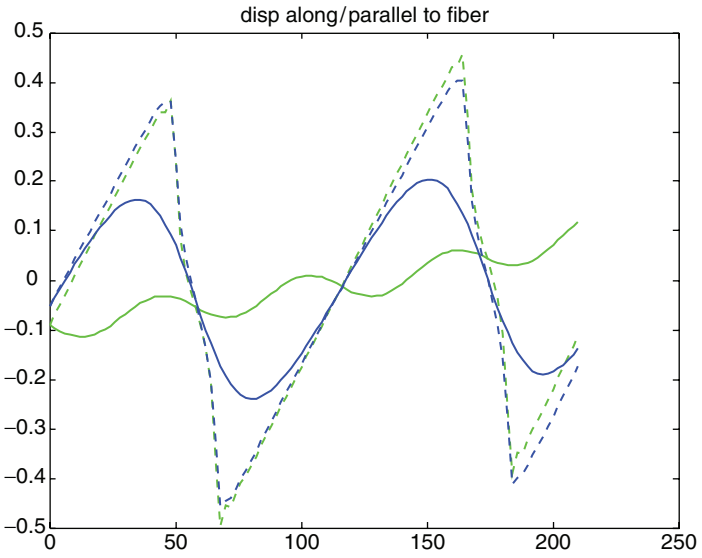

Fig. 3.15 Displacement field parallel to fibre axis $(\mathrm{L} = 100\,\mathrm{R})$ with and without overlap

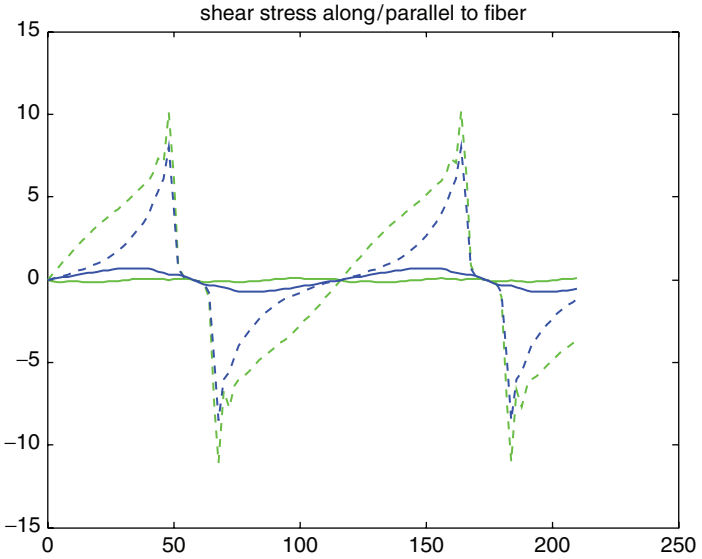

Fig. 3.16 Shear stress parallel to fibre axis $(\mathrm{L} = 100\,\mathrm{R})$ with and without overlap

boundary are satisfied, and (2) the numerical stability of the fictive source functions. Instability of the source functions can be observed in the end parts of fibres and between the discontinuous parts of source functions (Fig. 3.9). The instability in the end parts can result in inaccurate estimation of forces in fibre cross-section. The instability shown in the Fig. 3.9 does not influence the results greatly. It was observed

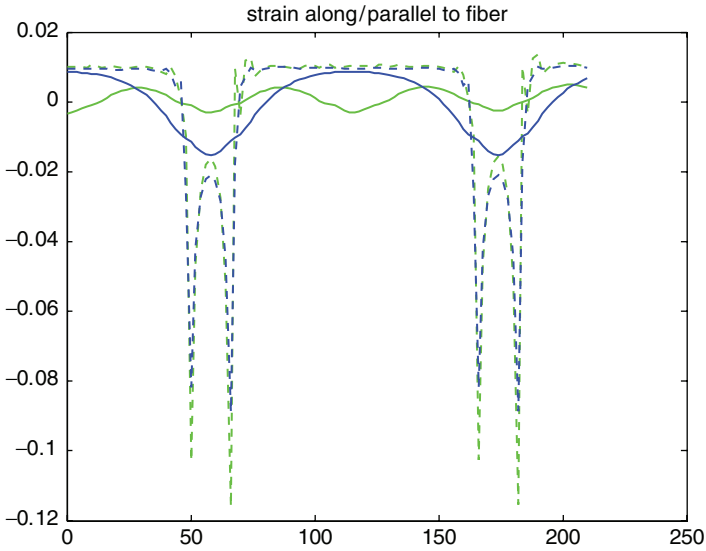

Fig. 3.17 Strain in fibre direction parallel to fibre axis (L = 100R) with and without overlap

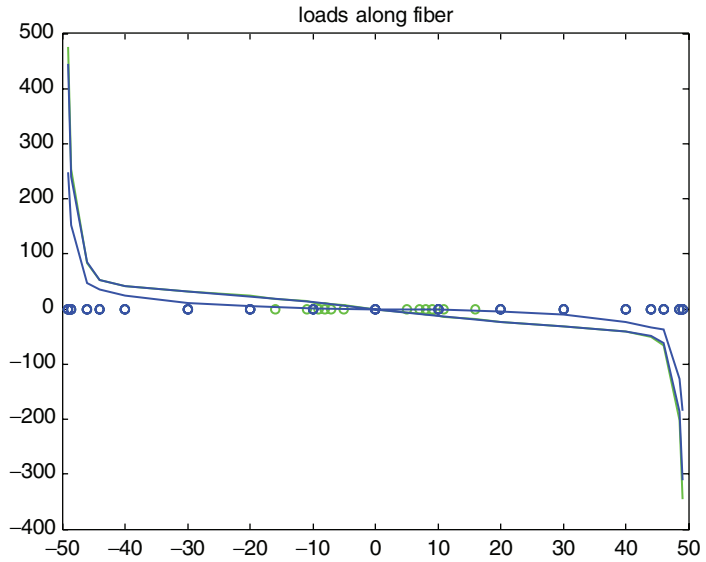

Fig. 3.18 Intensity of fictive forces along fibre (L = 100R) with and without overlap

that too fine 1D elements in the parts of fibres with large gradients can lead to instability of the source functions whereas too course elements decrease the accuracy of the primary variables. Both these features can destroy the accuracy of estimation of secondary fields (stresses, strains, forces in fibre cross section). No general rule has yet been found for choosing the nodal points for 1D source distribution.

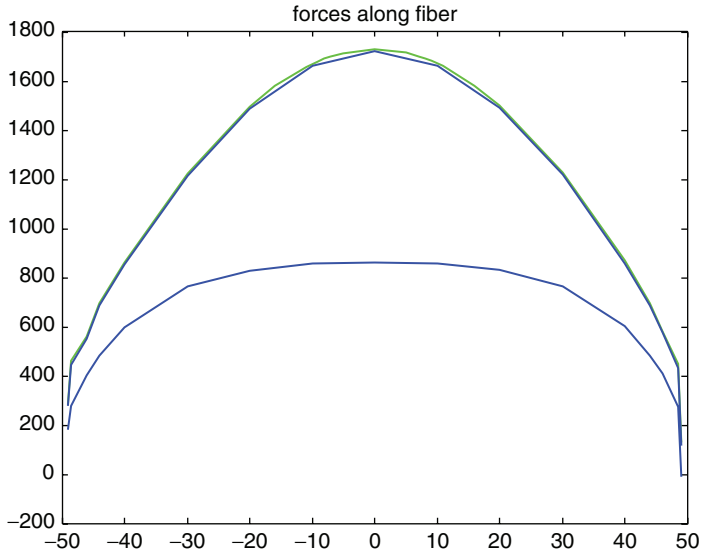

Fig. 3.19 Forces in fibre cross section $(L = 100R)$ with and without overlap

Extreme shear forces between the fibre and the matrix can lead to de-bonding of the fibre or to de-cohesion and re-cohesion at the ends and also in the middle of a fibre close to another fibre in materials reinforced with nanotubes, which are typical and very efficient novel reinforcing materials. This middle part of the fibre will carry the largest forces, which can lead to fracture of the fibre. The forces in the fibre can exceed the largest stresses in the matrix and the bonding stresses on the matrix-fibre interface by several orders.

3.4 Conclusions

The MCSF enables us to simulate the interactions both of matrix with stiff reinforcing fibres and of fibre with other fibres very effectively. Computational experiments have shown that very large gradients in all fields occur not only in the end parts of fibres, but also in points close to the ends of neighbouring fibres, more precisely in points on the line perpendicular to the axis of the neighbouring fibre. The large gradients in the end parts of fibres also influence numerical models. If polynomial interpolation of source functions is chosen in the models then finer division of the continuous function needs to be defined in these parts.

Numerical models used for simulation of all matrix-fibre and fibre-fibre interactions must maintain the gradients in order to correctly estimate the interactions. Because methods using volume discretization such as FEM and finite volume method (FVM) can smooth out the gradients, very fine meshes would be necessary for numerical models.

The extreme shear forces between fibre and matrix can lead to de-bonding or to de-cohesion in the end parts and also in the middle of a fibre close to another fibre in materials reinforced with fibres or nanotubes, which are typical and very efficient novel reinforcing materials. This middle part of the fibre will be subjected to the largest forces, which can lead to its fracture.

The forces in the fibre can result in stresses which can be larger by several orders than the largest stresses in the matrix, or in the bonding on the matrix-fibre interface. The optimal aspect ratio of fibres can be found for specific working stress/strain conditions in each part of a structure according to the strength of all fibre, matrix and bond between fibre and matrix. This is another attractive property of this kind of composite material.

Two types of problems simulated in our experiments show, as expected, that overlapping fibres reinforce the matrix more effectively. Fibres distributed without overlap can suffer breakage when subjected to high tension.

In the present model we have considered straight fibres, rigid in the axial direction. It is not complicated to consider some more general cases, using this model as the first step in the iteration process. However, more effort will be necessary to include features like boundary conditions for more complex shaped regions, curved fibres, nonlinear effects in matrix, and bonding properties.

Acknowledgements This research was partially supported by grands APVT-20-035404 and NATO RTA 001-AVT-SVK. The first two authors thank for this support.

References

1. Atieh MA et al. (2005) Multi-wall carbon nanotubes/Natural rubber nanocomposites. *Azo-Nano – Online Journal of Nanotechnology*, 1, pp. 1–11
2. Balaš J, Sládek J and Sládek V (1989) *Stress Analysis by Boundary Element Methods*. Elsevier, Amsterdam
3. Belytschko T, Liu WK and Moran B (2000) *Nonlinear Finite Elements for Continua and Structures*. Wiley, Chichester
4. Blokh VI (1964) *Theory of Elasticity*. University Press, Kharkov
5. Brebbia CA, Telles JCF and Wrobel LC (1984) *Boundary Element Techniques – Theory and Applications in Engineering*, Springer, Berlin
6. Cheng AHD and Cheng DT (2005) Heritage and early history of the boundary element method. *Journal of Engineering Analysis with Boundary Elements*, 29, pp. 268–302
7. Fu Y, Klimkowski KJ and Rodin GJ (1998) A fast solution method for three-dimensional many-particle problems in linear elasticity. *International Journal for Numerical Methods in Engineering*, 42, pp. 1215–1229
8. Gaul L and Moser F (2002) A Hybrid Boundary Element Approach Without Singular Boundary Integrals. In: *Selected Topics in Boundary Integral Formulations for Solids and Fluids*, Kompiš V. (ed.), Springer, Wien, pp. 107–116
9. Golberg MA and Chen CS (1998) The Method of Fundamental Solutions for Potential, Helmholtz and Diffusion Problems. In: *Boundary Integral Methods – Numerical and Mathematical Aspect*, Golberg MA. (ed.), Computational Mechanics, Southampton, pp. 103–176
10. Gomez JE and Power H (1997) A multipole direct and indirect BEM for 2D cavity flow at low Reynolds number. *Journal of Engineering Analysis with Boundary Elements*, 19, pp. 17–31

11. Greengard FL and Rokhlin V (1987) A fast algorithm for particle simulations. *Journal of Computational Physics*, 73, pp. 325–348
12. Jirousek J and Wroblewski A (1997) T-elements: State of the art and future trends. *Archives of Applied Mechanics*, 3, pp. 323–434.
13. Kachanov M, Shafiro B and Tsukrov I (2003) *Handbook of Elasticity Solutions*. Kluwer, Dordrecht
14. Karageorghis A and Fairweather G (1989) The method of fundamental solutions for the solution of nonlinear plane potential problems. *IMA Journal Numerical Analysis*, 9, pp. 231–242
15. Kompiš V and Štiavnický M (2006) Trefftz functions in FEM, BEM and meshless methods. *Computer Assisted Mechanics and Engineering Sciences*, 13, pp. 417–426
16. Kompiš V, Kompiš M, Kaukič M and Hui D (2006) Singular Trefftz Functions for Modelling of Material Reinforced by Hard Particles. *Proceedings of the Fifth International Conference on Engineering Computational Technology*, Topping, B.H.V., Montero, G. and Montenegro, R. (eds.), CD-ROM, Civil-Comp Press, Dun Eaglais
17. Kompiš V, Kompiš M and Kaukič M (2007) Method of continuous dipoles for modeling of materials reinforced by short micro-fibers. *Journal of Engineering Analysis with Boundary Elements*, 31, pp. 416–424
18. Ma H and Qin QH (2007) Boundary point method for linear elasticity based on direct formulations of conventional and hypersingular boundary integral equations, *Computers and Mathematics with Applications*, submitted
19. Mammoli AA and Ingber MS (1999) Stokes flow around cylinders in a bounded two-dimensional domain using multipole-accelerated boundary element method. *International Journal of Numerical Methods in Engineering*, 44, pp. 897–917
20. Mukherjee S (2002) The Boundary Contour Method. In: *Selected Topics in Boundary Integral Formulations for Solids and Fluids*, Kompiš V (ed.), Springer, Wien, pp. 117–150
21. Mukherjee S (2002) The Boundary Node Method. In: *Selected Topics in Boundary Integral Formulations for Solids and Fluids*, Kompiš V (ed.), Springer, Wien, pp. 151–180
22. Mukherjee S and Mukherjee YX (1998) The hypersingular boundary contour method for three dimensional elasticity, *ASME Journal of Applied Mechanics*, 65, pp. 300–309
23. Nishimura N (2002) Fast multipole accelerated boundary integral equations. *Applied. Mechanics Review*, 55, pp. 299–324
24. Nishimura N, Yoshida K and Kobayashi S (1999) A fast multipole boundary integral equation method for crack problems in 3D. *Journal of Engineering Analysis with Boundary Elements*, 23, pp. 97–105
25. Oden JT et al. (2006) *Simulation – Based Engineering Science: Revolutionazing Engineering Science Through Simulation*. Report NSF Blue Ribbon Panel
26. Peirce AP and Napier JAL (1995) A spectral multipole method for efficient solution of large-scale boundary element models in elastostatics. *International Journal for Numerical Methods in Engineering*, 38, pp. 4009–4034
27. Qin QH (2002) *The Trefftz Finite and Boundary Element Method*. WIT, Southampton
28. Štiavnický M, Kompiš V, Kaukič M (2007) Global dipole model for composite reinforced by micro/nano particles. *International Conference on Computational Modeling and Experiments of the Composites Materials with Micro-and Nano-Structure*, May 28–31 2007, CD-ROM
29. Wang H, Qin QH and Kang YL (2005) A new meshless method for steady-state heat conduction in anisotropic problems and inhomogeneous media. *Archive of Applied Mechanics*, 74, pp. 563–579
30. Wang H and Qin QH (2006) A meshless method for generalized linear and nonlinear Poisson-type problems. *Engineering Analysis wit Boundary Elements*, 30, pp. 515–521
31. Wang H, Qin QH and Kang YL (2006) A meshless model for transient heat conduction in functionally graded materials. *Computational Mechanics*, 38, pp. 51–60
32. Zhang JM, Tanaka M and Matsumoto T (2004) Meshless analysis of potential problems in three dimensions with the hybrid boundary node method. *International Journal for Numerical Methods in Engineering*, 59, pp. 1147–1160
33. Zienkiewicz OC and Taylor RL (2000)*The Finite Element Method*, 5th edn. Butterworth-Heinemann, Oxford